Theor Appl Genet (2014) 127:2415–2432
DOI 10.1007/s00122-014-2387-7

ORIGINAL PAPER

Mapping QTLs of yield-related traits using RIL population derived from common wheat and Tibetan semi-wild wheat

Gang Liu · Lijia Jia · Lahu Lu · Dandan Qin · Jinping Zhang · Panfeng Guan · Zhongfu Ni · Yingyin Yao · Qixin Sun · Huiru Peng

Received: 13 March 2014 / Accepted: 23 August 2014 / Published online: 11 September 2014

Abstract

Key message **QTLs controlling yield-related traits were mapped using a population derived from common wheat and Tibetan semi-wild wheat and they provided valuable information for using Tibetan semi-wild wheat in future wheat molecular breeding.**

Abstract Tibetan semi-wild wheat (*Triticum aestivum ssp tibetanum* Shao) is a kind of primitive hexaploid wheat and harbors several beneficial traits, such as tolerance to biotic and abiotic stresses. And as a wild relative of common wheat, heterosis of yield of the progeny between them was significant. This study focused on mapping QTLs controlling yield-related traits using a recombined inbred lines (RILs) population derived from a hybrid between a common wheat line NongDa3331 (ND3331) and the Tibetan semi-wild wheat accession Zang 1817. In nine location–year environments, a total of 148 putative QTLs controlling nine traits were detected, distributed on 19 chromosomes except for *1A* and *2D*. Single QTL explained the phenotypic variation ranging from 3.12 to 49.95 %. Of these QTLs, 56 were contributed by Zang 1817. Some stable QTLs contributed by Zang 1817 were also detected in more than four environments, such as *QPh-3A1*, *QPh-4B1* and *QPh-4D* for plant height, *QSl-7A1* for spike length, *QEp-4B2* for ears per plant, *QGws-4D* for grain weight per spike, and *QTgw-4D* for thousand grain weight. Several QTL-rich Regions were also identified, especially on the homoeologous group 4. The *TaANT* gene involved in floral organ development was mapped on chromosome 4A between *Xksm71* and *Xcfd6* with 0.8 cM interval, and co-segregated with the QTLs controlling floret number per spikelet, explaining 4.96–11.84 % of the phenotypic variation. The current study broadens our understanding of the genetic characterization of Tibetan semi-wild wheat, which will enlarge the genetic diversity of yield-related traits in modern wheat breeding program.

Introduction

Wheat is one of the most important food crops in the world, and wheat production will increasingly play a major role in world flood security for up to 8.9 billion people by 2030 (Brown 1994). However, wheat breeding faces the problem of yield plateaus, caused by narrow genetic basis of parental materials. The genetic diversity of cultivated common wheat is thought to be smaller than that of wild relatives due to founder effect that occurred during crop domestication (Ladizinsky 1985). Exploitation and utilization of the favorable alleles of wild relatives that were lost or weakened in cultivated wheat might be able to overcome the yield plateaus. And wild relatives or ancestors of wheat have been proven to be a valuable resource of beneficial alleles, and can be employed as a potential source for mining desirable alleles used in wheat breeding (e.g., Sheng

G. Liu and L. Jia contributed equally to this article.

Communicated by Xianchun Xia.

Electronic supplementary material The online version of this article (doi:10.1007/s00122-014-2387-7) contains supplementary material, which is available to authorized users.

G. Liu · L. Jia · L. Lu · D. Qin · J. Zhang · P. Guan · Z. Ni · Y. Yao · Q. Sun · H. Peng (✉)
State Key Laboratory for Agrobiotechnology and Key Laboratory of Crop Heterosis and Utilization (MOE), Key Laboratory of Crop Genomics and Genetic Improvement (MOA), Beijing Key Laboratory of Crop Genetic Improvement, National Plant Gene Research Centre (Beijing), China Agricultural University, Yuanmingyuan Xi Road NO. 2, Haidian district, 100193 Beijing, China
e-mail: penghuiru@cau.edu.cn

et al. 2012; Xie et al. 2012). Wild relatives have also been used successfully in tomato and rice breeding (Tanksley et al. 1996; Bernacchi et al. 1998; Moncada et al. 2001).

Tibetan semi-wild wheat is a kind of primitive hexaploid wheat that originated in the Tibet region of China, and is a close relative of wild progenitor of common wheat. However, the potential of Tibetan wheat in wheat yield improvement has not been well explored. Tibetan semi-wild shows spike disarticulation at maturity, whereas harbors many advantages, such as the tolerance abiotic stresses, tolerance to nutrition deficiency, which can be used in common wheat breeding (Sun et al. 1998). Recently, Wang (2010) conducted genetic analysis on eight agronomic traits using the recombinant inbred lines derived from the Tibetan semi-wild wheat Chayazheda29 and common wheat Yanzhan No.1, and the results revealed that these traits in the progeny populations showed transgressive segregation. Our previous study has also shown that the wide variation in grain number per spike (GNS) observed among F_2 population is retained in the recombinant inbred lines even when the parental values were not significantly different (data not shown). These results suggested that genetic loci (QTLs) affecting the agronomic traits are segregating, and that both Tibetan semi-wild wheat and common wheat contributed alleles for increased yield production. However, more efforts are needed to explore and identify favorable alleles from Tibetan wheat, which can be used in wheat yield improvement.

In the last two decades, using various segregating populations, QTLs controlling wheat yield and yield-related traits have been mapped and identified, such as plant height, spike length, spike number, the grain number of spike, floret number per spike, thousand grain weight (Li et al. 2007; Liao et al. 2008; Gaynor 2010; Sun et al. 2010; Ramya et al. 2010; Carter et al. 2011; Wang et al. 2011; Deng et al. 2011; Heidari et al. 2011; Cui et al. 2012, 2014). Some of these QTLs account for a large portion of the phenotypic variance and could be used for wheat yield improvement through molecular marker-assisted selection (MAS). MAS has been proved to be an important tool to accelerate the breeding program, and a prerequisite for MAS is the availability of molecular markers that are closely linked to the traits of interest (Hayes et al. 1993; Wang et al. 1994). However, few studies were conducted on detection of favorable yield-related QTLs from Tibetan semi-wild wheat.

After QTL mapping, the genes associated with some major QTLs were cloned by fine mapping, and gene-specific functional markers were developed and can be used for traits improvement. However, as a polyploidy species with a huge genome, it is difficult to identify individual yield-contributing genes in wheat through QTL mapping. Whereas gene-specific functional molecular marker, which is a new type of marker based on the association between sequence polymorphism and function of gene can be used directly in MAS, such as *TaVP1* involved in pre-harvesting sprouting resistance of wheat (Yang et al. 2007). *ANT* gene is a member of *AP2* gene family, *ANT* gene family from *Arabidopsis* has been proved to be associated with floral development, and *ANT* gene from wheat has been also related to ovule primordial at the floral organ development stage (Mizumoto et al. 2009). Polymorphic analysis and mapping of *TaANT* will be helpful for developing functional marker of this gene and using it in MAS of grain number per spike.

To better understand the genetic characterization of Tibetan semi-wild wheat for wheat improvement, a RIL population derived from common wheat ND3331 and Tibetan semi-wild wheat Zang 1817 was constructed and used to map QTLs controlling the yield components. The current study will provide valuable information for using Tibetan semi-wild wheat as a beneficial resource in future wheat molecular breeding.

Materials and methods

Materials and phenotyping

A population consisting of 217 ($F_{2:9}$) recombinant inbred lines derived from a hybrid between the common wheat line ND3331 and Tibetan semi-wild wheat accession Zang 1817 through single seed descent method was used in this study. The RIL population along with the two parental lines was phenotyped in Beijing from 2008 to 2011, in Shanxi from 2009 to 2011 and in Shandong from 2009 to 2010. The 9 year–location environments were designated as Beijing-2008 (E1), Beijing-2009 (E2), Shandong-2009 (E3), Shanxi-2009 (E4), Beijing-2010 (E5), Shandong-2010 (E6), Shanxi-2010 (E7), Beijing-2011 (E8), and Shanxi-2011 (E9), respectively. A randomized complete block design with three replications was employed for phenotyping in the field experiment. A spacing of 30 cm between rows and 6 cm between plants was maintained within a 2 m long row in single plot. The management of the field experiments was in accordance with local standard practices.

At maturity, ten randomly selected plants per genotype from each replication were used for phenotypic characterization, and the average value of the three replications was used for further analysis. Plant height (PH), spike length (SL) of the main spike and ears per plant (EP) were measured before harvesting, and the main spikes were bagged at the same time to measure the fertile spikelet number (FSN) and sterile spikelet number (SSN) (spikelet with one or more grains is considered to be fertile, on the contrary, spikelet with no grain is considered to be sterile), grain

weight per spike (GWS) and grain number per spike (GNS) after harvesting. Thousand grain weight (TGW) was measured after the seeds were totally dried. Floret number per spikelet (FNS) was calculated using the following formula: GNS/(FSN + SSN), indicating the mean of floret number per spikelet.

Construction of genetic linkage map and QTL analysis

A total of 2,500 markers were used to detect polymorphisms between the two parental lines, including microsatellite markers (Röder et al. 1998; Pestsova et al. 2000), EST-SSR marker DuPw (Eujayl et al. 2001). Xpsp markers were developed by University of Cambridge and Xcau markers developed by China Agricultural University. The 10 μL PCR reaction contained 1× buffer, 1.5 mM of $MgCl_2$, 0.2 mM of dNTPs, 20 ng of primers, 20 ng of genomic DNA and 1 unit of Taq polymerase. Amplification was conducted on Biometra DNA Thermal Cycler with 5 min at 94 °C initially, then 40 cycles of 45 s at 94 °C, 45 s at 50–70 °C for different primer pairs, and 90 s at 72 °C, and finally, 10 min at 72 °C for a final extension. The products were separated on 8 % polyacrylamide gels and visualized with silver staining. All marker data were scored by visual inspection and ambiguous bands were scored as missing genotype. The polymorphic markers were used for genotyping of the RIL population.

The genetic linkage map was constructed using Mapmaker/Exp version 3.0 (Lincoln et al. 1992) according to the protocol of the software. The threshold for log-likelihood (LOD) scores was set at 3.0 and genetic distances were calculated with the Kosambi function. Linkage groups were assigned to chromosomes and adjusted by comparing with published maps available on GrainGenes (http://wheat.pw.usda.gov/) and Triticarte (http://www.triticarte.com.au/) web sites and with a wheat consensus map (Somers et al. 2004).

Basic statistical analysis of the phenotypic data was performed by the software SPSS 13.0. Skewness and kurtosis were estimated from the phenotypic distribution of entry means to determine departure from normality. The ANOVA general linear model (GLM) analysis was performed to determine the significances of differences between parents and between nine environments. Broad-sense heritability was calculated using software QGA Station version 1.0 (http://ibi.zju.edu.cn/software/qga/) by the formula $h^2 = Vg/(Vg + (Vge)/e + Ve/re)$, in which the respective variance components are attributed to genotypic, genotype environment and experimental error effects, r is the number of replicates per environment, and e is the number of environments for a given trait. Phenotypic correlations were calculated for all combinations of traits on the basis of RIL means for each environment. QTL analysis was carried out by composite interval mapping (CIM) method using Windows QTL Cartographer 2.5 (Zeng 1993, 1994). Forward and backward regression was used to select cofactors for CIM with a threshold of $P < 0.05$. The parameters were as follows: background markers with 10, CIM model with 6, window size with 5 cM and permutation with default. A QTL was declared when the logarithm of the odds (LOD) score was greater than 2.5 in the overall mean dataset.

Mapping of the *TaANT* gene involved in floral organ development

Based on the cDNA sequence of *TaANT* (GB: AB458518), the genomic sequence of *TaANT* was obtained by aligning the cDNA to the genomic sequence of wheat variety Chinese spring released recently (http://www.cerealsdb.uk.net). Nine gene-specific primers were designed according to the DNA sequence and used for polymorphic analysis of genomic sequence between ND3331 and Zang 1817, and the polymorphic primer pair *TaANT8* was used as a genetic marker to map the *TaANT* gene on wheat genome (in formation of gene-specific primers are shown in Supplemental Table 1).

Results

Phenotypic variation of different traits

Averaged phenotypic variation for the nine traits of all the nine environments is presented in Table 1 (The phenotypic variation for the nine traits in each environment is presented in Supplemental Table 2, and the results of correlation analysis between the traits are shown in Supplemental Table 3). As shown in Table 1, five of the nine traits showed significant differences between the two parents ND3331 and Zang 1817, except for FSN, SSN, GNS and FNS. Among those five traits, PH of Zang 1817 was much higher than that of ND3331, EP of Zang 1817 was more than that of ND3331, SL of ND3331 was much longer than that of Zang 1817, and TGW and GWS of ND3331 were much higher than those of Zang 1817 (Table 1). Further analysis showed that all the nine traits segregated significantly and showed normal distribution in the RIL population. Transgressive segregation in the two parental lines was also observed (Table 1). For example, the maximum TGW for RIL No. 7 reached 47 g, which was 17.5 % higher than the higher parental line ND3331 (data not shown).

Different traits had quite different estimated heritability in this study (Table 1). The highest heritability was observed for PH, which could reach to 0.88, followed by SL (0.81), while SSN and EP had the lowest heritability (0.47 and 0.42, respectively), suggesting that these two

Table 1 Average variation and heritability of yield-related traits in the parental lines and RIL population across all environments

Trait	Parents		Population					
	ND3331	Zang1817	Max	Min	Aver	Kurt	Skew	h^2
PH (cM)	68.9 ± 7.9**	96.7 ± 8.6	99.1	28.7	70.5	0.2	−0.9	0.88
SL (cM)	13.2 ± 0.7**	11.2 ± 1.3	16.1	2.0	9.5	−0.8	−0.2	0.81
EP	8.1 ± 1.3*	11.9 ± 3.3	14.6	3.9	8.9	−0.2	0.2	0.42
FSN	19.5 ± 2.4	19.9 ± 3.7	23.5	14.0	18.4	0.1	−0.2	0.68
SSN	1.2 ± 0.5	1.3 ± 0.5	1.8	0.1	0.8	−0.1	0.6	0.47
GNS	65.2 ± 5.9	59.6 ± 6.5	85.5	44.1	64.2	−0.3	0.0	0.57
TGW (g)	40.6 ± 4.3**	26.7 ± 3.5	41.2	17.2	29.7	0.2	0.1	0.67
GWS (g)	2.4 ± 0.5**	1.4 ± 0.3	3.0	1.1	1.9	1.2	0.5	0.56
FNS	3.2 ± 0.3	3.0 ± 0.3	6.1	2.4	3.9	0.4	0.2	0.48

* and ** indicate significant differences between Zang 1817 and ND 3331 at $P = 0.05$ and 0.01, respectively

traits were sensitive to environment. The average heritability of FSN, TGW, GNS, GWS, and FNS was 0.68, 0.67, 0.57, 0.56, and 0.48, respectively.

Genetic linkage map construction

Out of the 2,500 markers analyzed, 335 markers showed polymorphism between the parents, and finally 274 co-dominant SSR and 41 EST-SSR were mapped on the genetic linkage map, distributing across all the 21 chromosomes, and spanning 2994.5 cM with the average spacing of 9.4 cM, and the total length of genetic distance for A, B and D genomes was 1,207.1, 854.4 and 933, respectively. The number of loci per linkage group ranged from 3 to 27 (Supplemental Table 4).

Chromosome regions associated with QTLs for yield-related traits

A total of 148 QTLs with LOD >2.5 were detected for the nine traits across the nine location–year environments, distributed on 19 chromosomes except for 1A and 2D (Table 2; Fig. 1). The number of QTLs on each chromosome ranged from 21 (4B) to 2 (7D). Some QTLs were consistently detected on the same marker across the nine location–year environments, such as *QPh-4D, QTgw-4D, QSl-7A1,* etc. As expected, QTLs contributed by the Tibetan semi-wild wheat Zang 1817 have been detected for all nine traits, such as *QPh-3A1*, *QEp-4B2* and *QGws-4D*, etc.

Plant height (PH)

A total of 15 QTLs were detected for plant height and mapped on chromosomes 1B, 2A, 2B, 3A, 4A, 4B, 4D, 5B, 5D, 7B, and 7D (Table 2; Fig. 1). Among these QTLs, *QPh-4D* located between *Xbarc1118* and *Xbarc105* on chromosome 4D was detected in all the nine environments, explained 26.82–49.95 % of the phenotypic variation, and the positive alleles were contributed by Zang 1817. *QPh-3A1* in the interval of *Xksm28-Xwmc428* on chromosome 3A was detected in five environments (E2, E3, E4, E6 and E7). It accounted for 5.44–7.18 % of the phenotypic variation. Another two QTLs located in the interval of *Xcau603-Xbarc1174b* (*QPh-4B1*) and *Xgwm513-Xksm154* (*QPh-4B3*) on chromosome 4B were detected in four and two environments (E2, E4, E6, E9 and E3, E6), respectively. And the phenotypic variation they explained was from 3.12 to 6.51 %, respectively. Furthermore, the positive alleles of all the four QTLs mentioned above were contributed by Zang 1817. Meanwhile, we also identified QTLs for PH that was contributed by the ND3331, such as *Qph-5D* in the interval of *Xbarc44-Xcfd8* on chromosome 5D and *Qph-2B* between *Xksm74* and *Xwmc344* on 2B.

Spike length (SL)

A total of 15 QTLs distributed on 12 chromosomes, including 1D, 2B, 3A, 3D, 4A, 4B, 4D, 5A, 5B, 5D, 6A, and 7A, for SL were detected in this study (Table 2; Fig. 1). Three major QTLs were detected for the trait. Of them, *QSl-7A1* flanked by the markers *Xcfd2049* and *Xcfd2028* on chromosome 7A with the additive effect ranged from 0.52 to 0.64 were detected in four environments (E1, E2, E6 and E7) and the explained phenotypic variation ranging from 7.5 to 10.84 %. Another QTL (*QSl-5A1*) on chromosome 5A, mapped in interval of *Xbarc261-Xbarc151*, explained the phenotypic variation ranged from 9.29 to 26.95 %. The positive alleles of the above two QTLs were contributed from Zang 1817. A stable QTL (*QSl-7A2*) from ND3331 on chromosome 7A located in interval of *Xpk39-Xbarc1167* was detected in two environments (responsible for phenotypic variation of 5.03 % in E6 and 13.85 % in E7), and additive effects were 0.38 and 0.55, respectively.

Ears per plant (EP)

Fourteen QTLs, including three major QTLs for EP, were detected on 10 chromosomes, including 1B, 2B, 3A,

Table 2 Interval, additive effects and contribution rate of QTL for yield-related traits in different environments

Traits	QTL	Interval	Position[a]	Environments	Additive effect[b]	R^2 (%)	QTL reported[c]
Plant height (PH)	*QPh-1B*	*Xgwm259-Xwmc44*	0	E9	2.52	3.79	
	QPh-2A	*Xh3-Xbarc296*	10	E2/E9	−3.35/−2.53	6.42/3.73	
	QPh-2B	*Xksm74-Xwmc344*	16	E5/E7	3.85/4.23	15.72/12.28	
	QPh-3A1	*Xksm28-Xwmc428*	6	E2/E3/E4/E6/E7	−3.07/−3.45/−3.02/−3.07/−3.27	5.44/7.09/6.09/5.88/7.18	
	QPh-3A2	*Xbarc1040-wmc88a*	0	E8/E9	−2.76/−2.56	6.43/3.95	
	QPh-4A	*Xwmc468-xbarc236*	4.5	E3/E4	−2.71/−2.91	4.27/5.36	
	QPh-4B1	*Xcau603-Xbarc1174b*	0.1	E2/E4/E6/E9	−2.8/−2.66/−2.94/−2.34	4.17/4.31/4.94/3.12	
	QPh-4B2	*Xbarc20-Xcau603*	10	E3	−3.68	7.43	
	QPh-4B3	*Xgwm513-Xksm154*	2	E3/E6	−3.4/−2.62	6.51/4.04	
	QPh-4D	*Xbarc1118-Xbarc105*	18	E1/E2/E3/E4E5/E6/E7/E8/E9	−6.81/−9.5/−8.22/−8.12/−4.79/−8.53/−6.36/−5.68/−8.42	30.83/49.95/36.63/42.92/23.63/43.39/27.11/26.82/40.2	
	QPh-5B1	*Xwmc386-Xcwem43*	0	E1	−2.46	4.11	
	QPh-5B2	*Xbarc4-Xbarc109*	0	E5	−2	4.22	
	QPh-5D	*Xbarc44-Xcfd8*	6	E2/E4/E9	3.3/3.6/3.1	6.29/8.59/5.92	
	QPh-7B	*Xgwm297-Xbarc72*	0	E8	−2.46	4.17	
	QPh-7D	*Xcau531-Xksm47*	0	E2/E4	2.66/2.43	4.87/3.9	
Spike length (SL)	*QSl-1D*	*Xpk54-Xwmc432*	0	E9	0.4	4.04	
	QSL-2B	*Xksm74-Xwmc344*	18	E4/E9	0.62/0.65	11.16/11.33	
	QSl-3A	*Xbarc321-Xwmc532*	8	E6	0.39	5.55	
	QSl-3D	*Xgdm72-xcfd64*	2	E4	0.47	6.29	
	QSl-4A	*Xwmc89-Xbarc224*	0.1	E3	0.36	4.62	
	QSl-4B1	*Xbarc20-Xcau603*	6	E6	0.63	13.15	
	QSl-4B2	*Xgwm513-Xksm154*	0	E6	0.55	9.35	
	QSl-4D	*Xbarc1118-Xbarc105*	22	E3	0.52	9.23	
	QSl-5A1	*Xbarc261-Xbarc151*	34	E4/E7/E9	−0.65/−0.45/−1.01	12.4/9.29/26.95	
	QSl-5A2	*Xbarc151-Xbarc1182b*	6	E5	−0.44	6.01	
	QSl-5B	*Xbarc142-Xbarc349*	0	E4	0.58	9.51	
	QSl-5D	*Xbarc44-Xcfd8*	8	E2	0.46	7.17	
	QSl-6A	*Xwmc201-Xgwm570*	0.1	E7	0.36	5.93	
	QSl-7A1	*Xcfd2049-xcfd2028*	0	E1/E2/E6/E7	−0.61/−0.62/−0.64/−0.52	7.5/8.66/10.84/7.84	
	QSl-7A2	*Xpk39-Xbarc1167*	28	E6/E7	0.38/0.55	5.03/13.85	
Ears per plant (EP)	*QEp-1B*	*Xbarc1158a-Xcfd65b*	0	E7	−0.28	4.02	
	QEp-2B1	*Xwmc314-Xcau375*	22	E2	0.51	5.76	
	QEp-2B2	*Xwmc314-Xcau375*	16	E3	0.86	8.23	
	QEp-3A	*Xgwm480-Xcfa2183*	24	E2	−0.53	6.29	
	QEp-4B1	*Xgwm513-Xksm154*	2	E1/E3/E4	−0.78/−1.27/−0.63	5.18/16.53/9.82	

Table 2 continued

Traits	QTL	Interval	Position[a]	Environments	Additive effect[b]	R^2 (%)	QTL reported[c]
	QEp-4B2	*Xbarc20-Xcau603*	6	E3/E4/E6/E9	−1.31/−0.63/−0.95/−0.4	17.05/9.91/24.98/8.43	
	QEp-4B3	*Xksm154-Xwmc349*	0	E7	−0.4	8.51	
	QEp-5A	*Xwmc467-Xcau20*	0	E1	−0.77	5.46	
	QEp-5B1	*Xcau129-Xgwm604*	10	E6/E9	0.64/0.58	11.82/17.89	
	QEp-5B2	*Xbarc142-Xbarc349*	6	E7	0.34	6.22	
	QEp-5D	*Xcfd8-Xcfd57b*	22	E9	−0.35	4.84	
	QEp-6B	*Xksm107-Xksm106*	0	E6	−0.38	4.14	
	QEp-7A	*Xcfd2049-Xcfd2028*	0	E2	0.68	6.81	
	QEp-7B	*Xcau30-Xgwm66c*	2	E7	−0.4	8.33	
Fertile spikelet number (FSN)	*QFsn-1D*	*Xbarc150-Xcfd65a*	6	E4	−0.52	7.31	
	QFsn-2A1	*Xgwm515-Xgwm473*	6	E1/E2/E8	−0.59/−0.62/−0.49	7.64/8.51/8.96	
	QFsn-2A2	*Xgwm473-Xbarc220*	0	E5/E7	−0.61/−0.58	6.57/7.56	
	QFsn-2A3	*Xbarc220-Xgwm95*	0	E9	−0.56	5.39	
	QFsn-2B	*Xksm74-Xwmc344*	14	E5/E7/E8	0.97/0.86/0.69	18.96/19.03/18.68	
	QFsn-4A1	*ANT-Xcfd6*	0	E5	−0.47	4.36	
	QFsn-4A2	*Xbarc28b-Xcau195*	0	E9	−0.71	9.21	
	QFsn-4B	*Xbarc20-Xcau603*	2	E2/E6	0.5/0.61	5.24/10.8	
	QFsn-6D	*Xbarc54-Xcfd132*	8	E1/E6	0.68/0.45	10.3/5.8	
	QFsn-7A1	*Xwmc488-Xcau483*	0	E2	−0.58	7.62	Quarrie et al. (2006)
	QFsn-7A2	*Xbarc1182a-Xbarc292*	4	E3	−0.54	6.2	
	QFsn-7A3	*Xcfd2049-xcfd2028*	4	E7	−0.66	8.31	
	QFsn-7D	*Xksm47-Xcfa2226*	0	E4	0.41	4.64	
Sterile spikelet number (SSN)	*QSsn-1B1*	*Xbarc1131-Xbarc1158a*	4.1	E1/E6	0.16/0.2	6.8/7.31	
	QSsn-1B2	*Xcewm9-Xgwm666*	6.1	E1/E6	0.16/0.22	6.63/8.93	
	QSsn-1B3	*Xbarc8-Xcfa2241b*	0	E2	0.17	4.92	
	QSsn-1D	*Xgdm19-Xwmc216*	18	E2/E9	0.2/0.17	7.92/8.18	
	QSsn-2A	*Xgwm425b-Xgwm515*	0	E5	−0.06	5.86	
	QSsn-2B	*Xksm74-Xwmc344*	0	E7/E8	0.12/0.19	10.09/13.9	
	QSsn-3D1	*Xgdm28-Xgdm8*	2	E1	−0.22	10.52	
	QSsn-3D2	*Xgdm8-Xgdm72*	0	E2/E4	−0.24/−0.42	11.63/7.68	
	QSsn-4A1	*Xwmc161-Xbarc1158b*	2	E4	0.33	4.64	
	QSsn-4A2	*Xxwmc491-Xbarc1052*	0	E7	0.1	7.18	
	QSsn-4A3	*XANT-Xcfd6*	0	E9	0.17	7.71	
	QSsn-4B1	*Xcau603-Xbarc1174b*	0.1	E2	−0.18	5.88	

Table 2 continued

Traits	QTL	Interval	Position[a]	Environments	Additive effect[b]	R^2 (%)	QTL reported[c]
	QSsn-4B2	*Xksm154-Xwmc349*	0	E2/E6	−0.19/−0.17	7/5.25	
	QSsn-4B3	*Xbarc20-Xcau603*	2	E3/E6/E9	−0.26/−0.26/−0.18	9.09/12.52/8.34	
	QSsn-4D	*Xbarc105-Xbarc217*	0	E4/E9	−0.32/−0.18	4.16/8.44	
	QSsn-5A1	*Xbarc151-Xbarc1182b*	8	E8	−0.24	10.86	
	QSsn-5A2	*Xbarc351-Xgwm186*	0.1	E8	0.17	3.93	
	QSsn-6A	*Xwmc201-Xgwm570*	0.1	E9	0.14	4.93	
	QSsn-6B1	*Xcau440-xbarc361*	0	E4	0.53	7.34	
	QSsn-6B2	*Xgwm680-Xgwm518*	0	E7	0.12	9.15	
	QSsn-7A	*Xcfd2123-Xgwm63*	26.1	E1	0.14	5.06	
	QSsn-7B1	*Xgwm297-Xbarc72*	0	E1/E6/E8	−0.14/−0.15/−0.11	4.83/4.26/5.25	
	QSsn-7B2	*Xbarc72-Xcfa2174a*	2	E2/E4	−0.19/−0.47	7.05/9.49	
	QSsn-7B3	*Xbarc65-Xgwm297*	2	E5	−0.06	6.56	
Grain number per spike (GNS)	*QGns-2B1*	*Xcfd283-Xgwm501*	0	E1/E5/E7	2.99/2/2.61	5.94/4.56/6.91	Hai et al. (2008)
	QGns-2B2	*Xgwm501-Xcau68*	0	E6/E9	2.17/2.2	5.29/5.44	Hai et al. (2008)
	QGns-2B3	*Xksm74-Xwmc344*	0	E9	1.98	4.55	
	QGns-3D	*Xwmc375-Xgwm645*	0.1	E8	−1.98	5.26	
	QGns-4A	*Xcau577-Xcwem34*	0	E2/E3	2.45/2.32	3.95/3.76	
	QGns-4B	*Xbarc20-Xcau603*	4	E2/E3/E6/E8/E9	3.13/3.43/3.66/2.26/2.43	7.67/11.39/14.25/6.33/6.41	Marza et al. (2006); Wang et al. (2011)
	QGns-4D	*Xbarc1118-Xbarc105*	8	E4/E8	3.69/2.67	9.76/9.29	
	QGns-5A	*Xwmc467-Xcau20*	0	E6/E8	1.95/1.65	4.27/3.59	
	QGns-5D	*Xksm59-Xbarc44*	0	E8	-1.78	4.03	
	QGns-6B	*Xwmc494-Xksm107*	6	E3	2.13	4.49	
	QGns-6D	*Xbarc54-Xcfd132*	10	E5	2.72	7.99	
	QGns-7A	*Xwmc488-Xcau483*	0	E9	-1.99	3.83	
	QGns-7B	*Xwmc273-Xbarc1073*	0	E8	1.97	4.85	
Grain weight per spike (GWS)	*QGws-2B*	*Xgwm501-Xcau68*	2	E9	0.11	5.64	
	QGws-3A	*Xgwm480-Xcfd2183*	16	E2	0.13	6.97	
	QGws-3B1	*Xgwm566-Xbarc1020*	0.1	E4	0.1	5.47	
	QGws-3B2	*Xw6-Xwmc231*	12	E7	0.09	5.19	
	QGws-4A1	*Xcau577-Xcwem34*	0	E2	0.13	5.55	
	QGws-4A2	*Xwmc491-Xbarc1052*	0	E6/E8	0.09/0.11	4.57/4.31	
	QGws-4B1	*Xgwm513-Xksm154*	2	E1/E3	0.13/0.07	6.8/7.72	
	QGws-4B2	*Xbarc20-Xcau603*	6	E2/E3/E6/E7	0.15/0.09/0.14/0.1	8.41/13.77/9.5/5.94	
	QGws-4B3	*Xksm154-Xwmc349*	0	E2/E6/E9	0.15/0.1/0.15	8.29/5.15/11.18	

Table 2 continued

Traits	QTL	Interval	Position[a]	Environments	Additive effect[b]	R^2 (%)	QTL reported[c]
	QGws-4D	*Xbarc105-Xbarc217*	0	E2/E3/E6/E7/E8	−0.13/−0.05/−0.1/−0.09/−0.12	6.16/4.4/5.49/4.45/5.2	
	QGws-5A1	*Xcau20-Xbarc28c*	0	E1/E4/E9	0.11/0.09/0.11	5.06/4.14/5.48	
	QGws-5A2	*Xbarc351-Xgwm186*	2	E5	0.09	6.29	
	QGws-5B1	*Xgwm604-Xbarc140*	2	E3	−0.06	6.79	
	QGws-5B2	*Xcau129-Xgwm604*	22	E6	−0.15	11.98	
	QGws-5D	*Xbarc44-Xcfd8*	4	E2	0.11	5.4	
	QGws-6B1	*Xksm107-Xksm106*	0	E2	0.11	5.02	
	QGws-6B2	*Xwmc494-Xksm107*	6	E3/E9	0.07/0.1	8.36/5.51	
	QGws-6D	*Xbarc54-Xcfd132*	4	E6	0.11	6.23	
	QGws-7B	*Xcau30-Xgwm66c*	2	E5	0.08	4.8	Mir et al. (2012); Cui et al. (2013)
Thous nd grain weight (TGW)	*QTgw-3A1*	*Xgwm480-Xcfd2183*	16	E2/E3/E4	1.62/0.82/1.23	9.59/6.93/10.67	
	QTgw-3A2	*Xbarc312-Xbarc322*	0	E5	1.19	4.84	
	QTgw-3B	*Xbarc1020-Xwmc505*	0	E9	1.13	4.96	
	QTgw-3D	*Xgwm645-Xcau569*	4	E3	0.75	5.76	
	QTgw-4A1	*Xwmc491-Xbarc1052*	0	E8	1.32	3.91	
	QTgw-4A2	*Xbarc28b-Xcau195*	0	E9	1.08	4.46	
	QTgw-4B1	*Xbarc20-Xcau603*	6	E1/E3/E9	1.36/0.71/1.51	7.08/4.75/9.4	Wang et al. (2011)
	QTgw-4B2	*Xcau603-Xbarc1174b*	0.1	E4/E8	0.86/1.43	4.86/4.41	Wang et al. (2011)
	QTgw-4D	*Xbarc1118-Xbarc105*	28	E2/E3/E4/E6/E7/E8/E9	−2.14/−1.6/−0.99/−1.9/−0.95/−2.97/−1.1	16.04/25.08/6.44/12.45/5.07/19.61/4.59	
	QTgw-5A1	*Xbarc351-Xgwm186*	0	E1/E2/E4/E5/E7/E9	1.12/1.23/1.01/1.78/1.57/1.28	4.97/5.57/7.2/10.89/14.25/6.48	
	QTgw-5A2	*Xbarc1182b-Xbarc330*	0	E3/E6	0.65/1.11	4.34/4.31	
	QTgw-5B	*Xcau129-Xgwm604*	20	E3/E6	−1.16/−2.28	13.78/18.58	
	QTgw-5D	*Xksm59-Xbarc44*	8	E7	1.07	6.66	
	QTgw-6A	*Xgwm334-Xgdm36*	0	E8	1.39	4.47	
	QTgw-7B	*Xcau30-Xgwm66c*	2	E5	1.31	5.68	Cui et al. (2013)

Table 2 continued

Traits	QTL	Interval	Position[a]	Environments	Additive effect[b]	R^2 (%)	QTL reported[c]
Floret number per spikelet (FNS)	*QFns-1B1*	*Xcau495-Xbarc188*	6	E5	−0.11	11.59	Peng et al. (2003); Wang et al. (2009); Zhang et al. (2012)
	QFns-1B2	*Xwmc44-xcau495*	2	E9	−0.07	4.54	
	QFns-1B3	*Xbrc1174a-Xbarc1131*	0	E9	−0.07	3.9	
	QFns-2A	*Xbarc296-Xgwm425b*	0	E8/E9	0.09/0.09	5.03/8.61	
	QFns-2B1	*Xgwm501-Xcau68*	2	E7	0.09	6.2	
	QFns-2B2	*Xcau68-Xcau319*	0	E9	0.06	3.66	
	QFns-3A	*Xbarc321-Xwmc532*	8	E2	0.09	5.5	
	QFns-4A1	*Xbarc28b-Xcau195*	0	E1/E2	0.13/0.13	8.09/11.84	Wang et al. (2011)
	QFns-4A2	*Xcau577-Xcwem34*	0	E3	0.1	7.17	Wang et al. (2011)
	QFns-4A3	*Xbarc1052-xwmc48*	0	E4	0.71	4.96	Wang et al. (2011)
	QFns-4A4	*ANT-Xcfd6*	0	E5/E6	0.07/0.09	5.01/5.43	Wang et al. (2011)
	QFns-4A5	*Xbarc224-Xksm71*	0	E7/E8	0.12/0.09	10.14/5.75	Wang et al. (2011)
	QFns-4A6	*Xgwm610-Xwmc491*	0	E8	0.09	5.12	Wang et al. (2011)
	QFns-4B1	*Xksm154-Xwmc349*	0	E2/E3/E6	0.11/0.08/0.09	7.73/4.48/5.11	
	QFns-4B2	*Xbarc20-Xcau603*	8	E3/E6	0.12/0.1	10.33/7.54	
	QFns-4B3	*Xcau603-Xbrc1174b*	0	E9	0.07	4.22	
	QFns-5B	*Xcwem43-Xbarc128*	3	E4	−0.69	5.27	
	QFns-5D	*Xcfd226-Xbarc161*	2	E4	−0.77	6.63	Zhang et al. (2012)
	QFns-6B	*Xwmc494-Xksm107*	6	E3	0.08	4.57	
	QFns-7B	*Xgwm297-Xbarc72*	0	E1/E6/E9	0.11/0.08/0.06	5.47/4.64/3.86	

[a] Position means the distance of LOD peak value for QTL after the first marker in the marker interval

[b] Positive values of the additive effect indicate that ND3331 alleles increase the corresponding trait, and, conversely, negative values indicate that Zang 1817 alleles increase it

[c] The comparison was performed when there were same makers in the QTL regions between our study and others'

4B, 5A, 5B, 5D, 6B, 7A, and 7B (Table 2; Fig. 1). *QEp-4B1* located on chromosome 4B is flanked by *Xgwm513* and *Xksm154* and was detected in E1, E3 and E4, which explained from 5.18 to 16.53 % of the total phenotypic variation with additive effect ranged from 0.63 to 1.27. *QEp-4B2* in the interval of *Xbarc20-Xcau603* was identified on the same chromosome in four environments (E3, E4, E6 and E9), with explained phenotypic variation being from 9.91 to 24.98 %. The favorable alleles of the two QTLs were both contributed by Zang 1817. Another major QTL (*QEp-5B1*), with the positive allele being from ND3331, was mapped in the interval of *Xcau129-Xgwm604* on chromosome 5B both in E5 and E9, explained 11.82–17.89 % of the phenotypic variation, respectively.

Fertile spikelet number (FSN)

Thirteen QTLs for FSN, mapped on chromosomes 1D, 2A, 2B, 4A, 4B, 6D, 7A and 7D, and nine of them had the positive alleles from Zang 1817 (Table 2; Fig. 1). One major QTL (*QFsn-2A1*) was consistently mapped in the interval of *Xgwm515-Xgwm473* on chromosome 2A in E1, E2 and E8, and explained the phenotypic variation ranged from 7.64 to 8.51 %. *QFsn-2A2* in a close proximity to *QFsn-2A1* was identified in the interval of *Xgwm473-Xbarc220* both in E5 and E7, explained 6.57–7.56 % of the phenotypic variation, respectively. Another two QTLs on chromosome 7A, *QFsn-7A1* in the interval of *Xwmc488-Xcau483* and *QFsn-7A2* in the interval of *Xbarc1182a-Xbarc29*, were detected in E2 and E3, respectively, and explained the phenotypic variation of 7.62–6.2 %. It was worthy to note that the markers *Xcau483* and *Xbarc1182a* were closely linked to each other (with a genetic distance of 0.3 cM), and presence of the two QTLs increased FSN and the positive allele were from Zang 1817.

Sterile spikelet number (SSN)

A total of 24 QTLs for SSN were detected on chromosomes 1B, 1D, 2A, 2B, 3D, 4A, 4B, 4D, 5A, 6A, 6B, 7A, and 7B in different environments (Table 2; Fig. 1). A major QTL (*QSsn-3D2*) was mapped between *Xgdm8* and *Xgdm72* on chromosome 3D in E2 and E4, The locus accounted for 11.63 and 7.68 % of the phenotypic variation, respectively. Another major QTL (*QSsn-3D1*) with explained phenotypic variation of 10.52 % was also detected in the vicinity of *Xgdm8* in E1. Two additional QTLs were mapped on chromosome 4B, *QSsn-4B2* mapped in the interval of *Xksm154-Xwmc349* was detected in E2 and E6 with the explained phenotype variation between 7 and 5.25 %, respectively. *QSsn-4B3* mapped in the interval of *Xbarc20-Xcau603* was detected in E3, E6 and E9 that explained 8.3–12.52 % of the phenotypic variation. Two QTLs were mapped close to *Xbarc72* on chromosome 7B: *QSsn-7B1* detected in E1, E6 and E8, explained 4.26–5.83 % of the phenotypic variation, and *QSsn-7B2* detected in E2 and E4, explained 7.05–9.49 % of the phenotypic variation, respectively. All the positive alleles of these QTL were derived from Zang 1817.

Grain number per spike (GNS)

Thirteen QTLs on chromosomes 2B, 4A, 4B, 4D, 5A, 5D, 6B, 6D, 7A, and 7B for GNS were identified in this study (Table 2; Fig. 1). A QTL (*QGns-2B1*) in the interval of *Xcfd283-Xgwm501* on chromosome 2B was detected in three environments (E1, E5 and E7), and another QTL, *QGns-2B2* close to *QGns-2B1* in the interval of *Xgwm501-Xcau68* was detected in E6. The genetic distance between the two QTLs and *Xgwm501* was 7.4 and 0 cM, respectively. The additive effect of the two QTLs ranged from 2.0 to 2.99, and explained from 4.56 to 6.91 % of the phenotypic variation. Another two QTLs, *QGns-4A* and *QGns-4B,* were located in the interval of *Xcau577-Xcwem34* on chromosome 4A and *Xbarc20-Xcau603* on 4B, respectively. *QGns-4A* could be detected both in E2 and E3, and additive effect was 2.45–2.32, respectively. It explained 3.95–3.76 % of the phenotypic variation. *QGns-4B* was detected in five environments (E2, E3, E6, E8 and E9), and with the explained phenotypic variation being from 6.33 to 14.25 %. All of those QTLs for this trait were from ND3331.

Grain weight per spike (GWS)

A total of 19 QTLs for GWS were identified on chromosomes 2B, 3A, 3B, 4A, 4B, 4D, 5A, 5B, 5D, 6B, 6D, and 7B (Table 2; Fig. 1). One major QTL (*QGws-4D*) mapped in the interval of *Xbarc105-Xbarc217* on chromosome 4D was detected in five environments (E2, E3, E6, E7 and E8), and explained from 4.40 to 6.16 % of total phenotypic variation. Zang 1817 contributed positive allele for three QTLs (*QGws-4D*, *QGws-5B1* and *QGws-5B2*). The positive alleles of three other QTLs (*QGws-4B1, QGws-4B2 and QGws-4B3*), which were mapped on chromosome 4B, explained 5.9–13.77 % of the phenotypic variation were contributed by ND3331.

Thousand grain weight (TGW)

For TGW, 15 QTLs distributed on 11 chromosomes were identified, including 3A, 3B, 3D, 4A, 4B, 4D, 5A, 5B, 5D, 6A, and 7B (Table 2; Fig. 1). A major QTL (*QTgw-4D*), located in the interval of *Xbarc1118-Xbarc105* on chromosome 4D in seven environments (E2, E3, E4, E6, E7, E8 and E9), could explain up to 25.08 % of the phenotypic

variation. Another major QTL (*QTgw-5B*) in the interval of *Xcau129-Xgwm604* on chromosome 5B was detected in E3 and E6, with additive effect being 1.16–2.28, respectively, and it explained 13.78–18.58 % of the total phenotypic variation, respectively. The two positive QTLs were derived from Zang 1817. Two major positive QTLs contributed by ND3331 were identified, including *QTgw-3A1* in the interval of *Xgwm480-Xcfd2183* on chromosome 3A identified in E2, E3 and E4, and *QTgw-5A1* in the interval *Xbarc351-Xgwm186* on chromosome 5A detected in six environments (E1, E2, E4, E5, E7, and E9). The two QTLs explained the phenotypic variation ranging from 6.93 to 10.67 % and from 4.97 to 14.25 %, respectively.

Floret number per spikelet (FNS)

In this study, we identified 20 QTLs for FNS located on chromosomes 1B, 2A, 2B, 3A, 4A, 4B, 5B, 5D, 6B, and 7B (Table 2; Fig. 1). Five major QTLs (*QFns-4A1, QFns-4A2*, *QFns-4A3*, *QFns-4A4* and *QFns-4A5*) were mapped in the vicinity of the gene-specific marker *ANT* in eight of the nine environments (Table 2; Fig. 1), with additive effect ranging from 0.07 to 0.71 and explained from 4.96 to 11.84 % of the total phenotypic variation. However, the positive QTL alleles were all from ND3331. Another QTL (*QFns-4B1*) was mapped in the interval of *Xksm154-Xwmc349* on chromosome 4B in E2, E3 and E6, with the explained phenotypic variation ranging from 4.48 to 7.73 %. Among the 20 QTLs identified for FNS, the positive alleles of 5 QTLs (*QFns-1B1, QFns-1B2, QFns-1B3, QTgw-5B* and *QTgw-5D*) were contributed by Zang 1817.

Mapping of *TaANT* gene involved in floral organ development

To map the *TaANT* locus in wheat genome, 9 gene-specific primer pairs covered the whole genomic sequence of *TaANT* were designed and used to analyze the polymorphism between ND3331 and Zang 1817 (Supplemental Table 1). The PCR product of the primer pair *TaANT8* in the seventh intron showed polymorphism between the two parents. Further sequencing of the polymorphic PCR products showed that there are an insertion of eight nucleotides in the genomic sequence of *TaANT* in ND3331 and an deletion of two nucleotides in Zang 1817 (data not shown). *TaANT* was mapped in the interval of *Xksm71-Xcfd6* on chromosome 4A. It was worthy to note that five major QTLs (*QFns-4A1*, *QFns-4A2*, *QFns-4A3* ,*QFns-4A4* and *QFns-4A5*) controlling FNS were mapped close to the gene-specific marker *ANT* in eight environments (Table 2; Fig. 1), with additive effect ranging from 0.07 to 0.71 and explaining from 4.96 to 11.84 % of total phenotypic variation.

Discussion

Tibetan semi-wild wheat can be used as valuable gene resource

Wild relatives of plants with extensive genetic diversity have the potential in QTL mapping, and the continued sampling of wild germplasms would result in new QTL/gene discovery (Tanksley and McCouch 1997). Wild relatives have been used successfully in breeding new crop cultivars mainly as sources of biotic and abiotic stress resistance or tolerance; however, not enough attention was paid to their use in yield improvement programs, since yield of them showed no advantages as compared to cultivated plants.

Tibetan semi-wild wheat originates from the Tibetan region of China, and is distinctly related to the cultivated hexaploid wheat. Our previous study showed that the average genetic distance between Tibetan semi-wild wheat and common wheat was larger than that between common wheat genotypes, and Tibetan semi-wild wheat can be used to broaden the genetic basis of common wheat in breeding programs (Sun et al. 1998).

The accession Zang 1817 of Tibetan semi-wild wheat used in this study performed poorly in the yield and yield-related traits as compared to the common wheat line ND3331; however, significant transgressive segregation was observed for all the traits analyzed. For example, SSN for ND3331 and Zang 1817 was 0.9 and 0.4 in E1, respectively, while SSN in the RIL population could reach to 3.5 in E1, similar results were also observed for other traits (Table 1). This suggested that the Tibetan semi-wild wheat Zang 1817 could be used to explore the favorable QTLs/genes which could be used to improve these traits in wheat breeding.

In this study, the RIL population derived from common wheat line ND3331 and Tibetan semi-wild wheat accession Zang 1817 was used to construct genetic linkage map and to map QTLs controlling yield-related traits. As expected, a total of 56 QTLs contributed positively by Zang 1817 have been detected for the nine traits, representing about 37.7 % of the total 148 QTLs detected (Table 2). *QPh-4D* for instance, detected in all the nine environments, explained about 26.82–49.95 % of the phenotypic variation of plant height. *QTgw-4D*, a QTL for thousand grain weight which was detected in seven environments, could explain up to 25.08 % of the phenotypic variation. *QEp-4B2* in the interval of *Xbarc20-Xcau603* which accounts for EP was identified on the same chromosome in four environments. And superior alleles of the two QTLs came from Zang 1817. These results suggested that Tibetan semi-wild wheat can be used as valuable gene resource in breeding wheat with high-yield potential. Thus, it was difficult to know if the detected QTL was a major QTL with larger

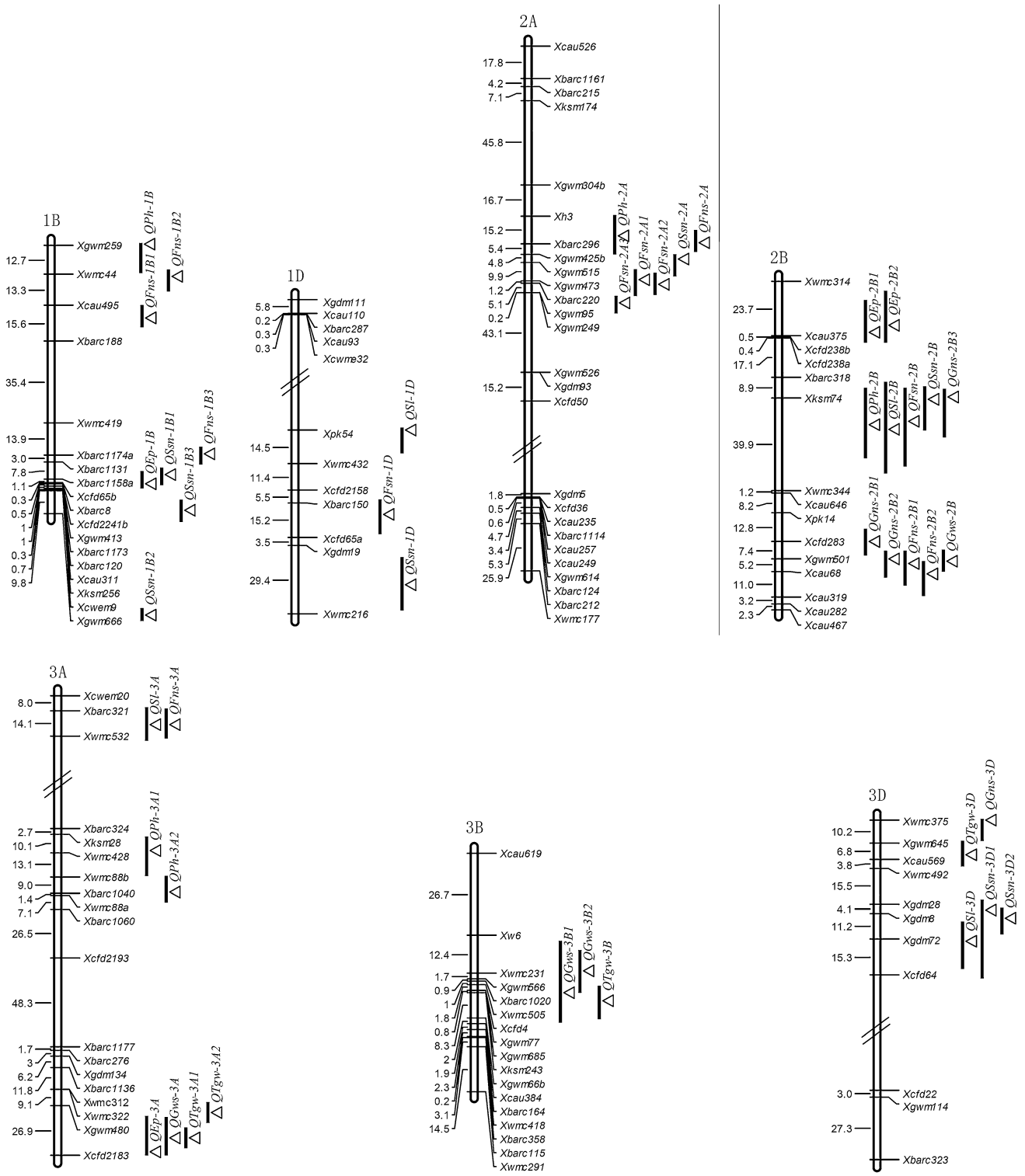

Fig. 1 QTLs for the yield-related traits of the RIL population. Map distances (cM) are indicated on the *left* of each chromrosome, and marker names are on the *right*. The LOD peak of each QTL is indicated by an *arrowhead* and the length of the bars indicates the QTL confidence interval with LOD values of more than 2.5

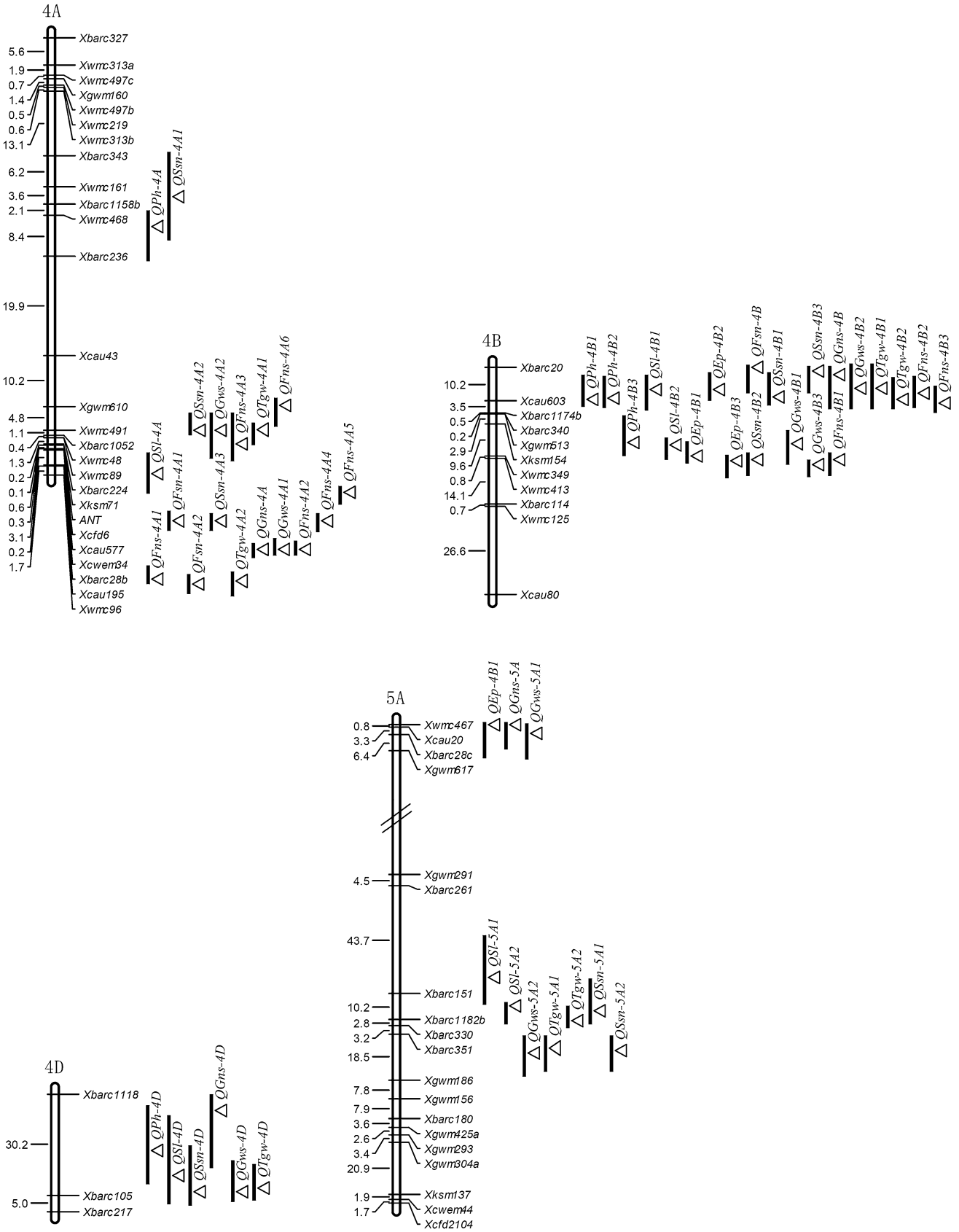

Fig. 1 continued

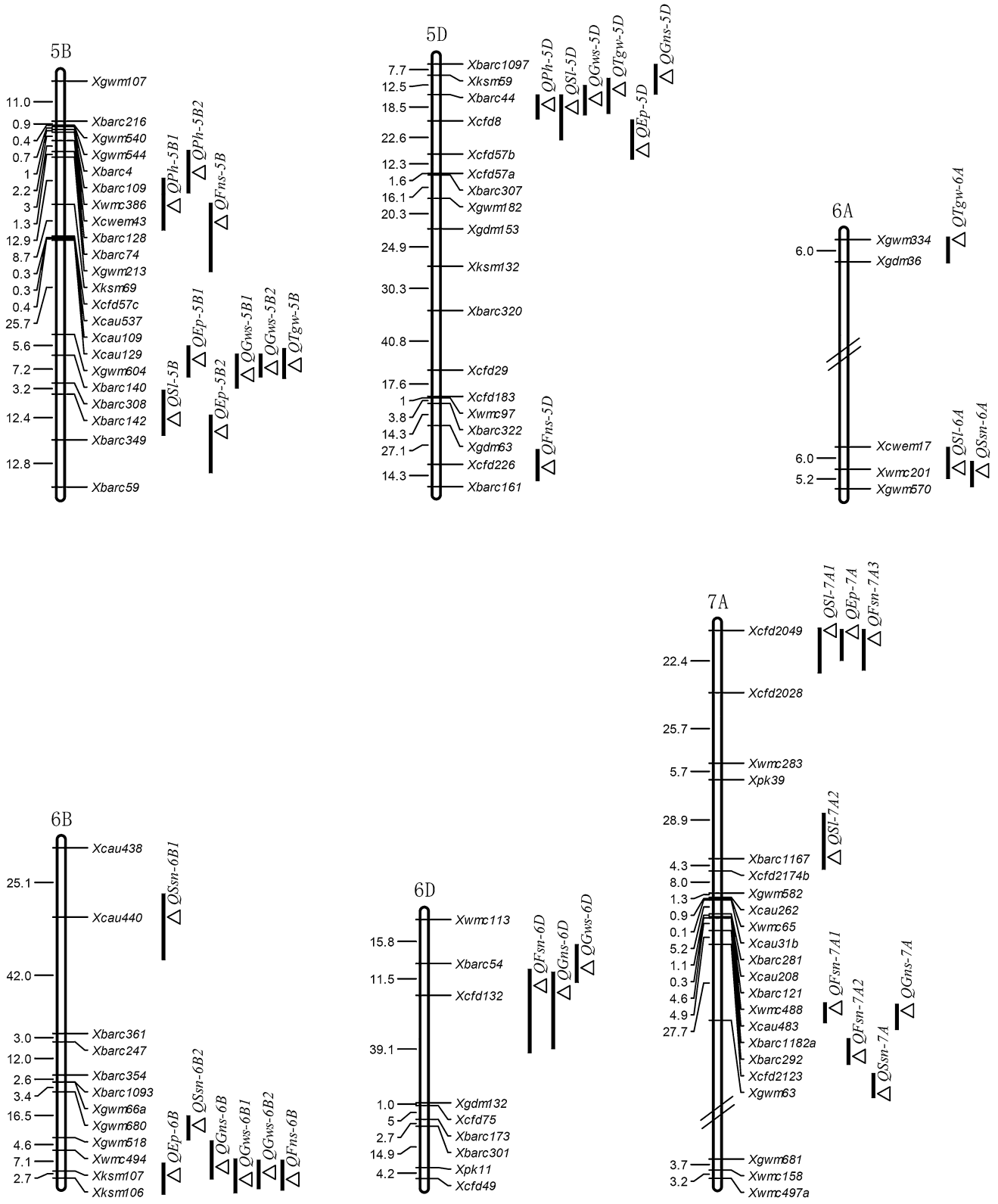

Fig. 1 continued

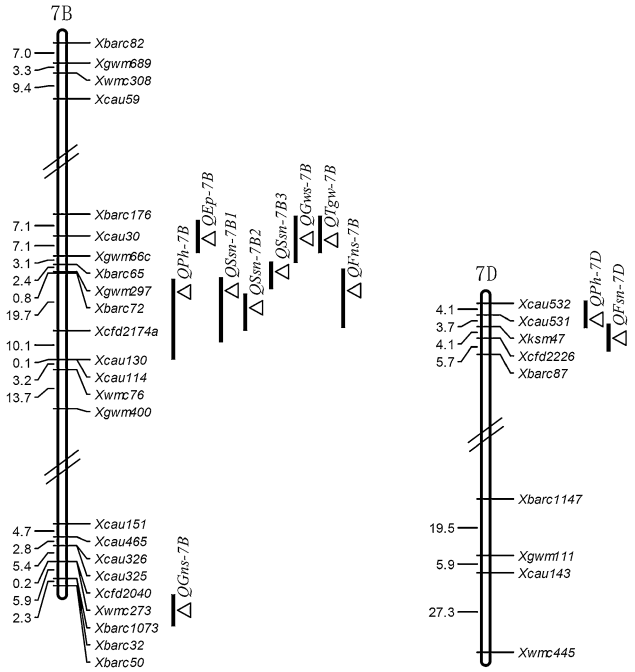

Fig. 1 continued

effect or several genes with smaller effects were contained. It was also difficult to dissect QTL into Mendelian factors. As a follow-up to this study, we have produced an AB-QTL population that represents a great opportunity to test the veracity of the putative QTLs of agronomically interesting alleles remaining in the wild species and fine mapping of the detected QTLs.

QTLs for yield-related traits detected in this study were mapped in the same interval previously

For comparison of our data and those of previous studies, we focused on the correspondences of loci that were based on the sharing of common markers with similar genetic positions on the linkage map (Table 2). Totally, 16 QTLs were found to be consistent between our data and other previous studies, and most of them were contributed by ND3331, except for *QFsn-7A1*, *QFns-1B1* and *QFns-5D* (Table 2). Two QTLs (*QTgw-4B1* and *QTgw-4B2*, explained 4.75–9.4 and 4.41–4.86 % of the phenotypic variation, respectively) for TGW were detected near the marker *Xcau603* on chromosome 4B, which may be the same locus for the trait. Wang et al. (2011) also found a QTL for TGW in the same region. In our study, a major QTL (*QTgw-4D*, explained 4.59–25.08 % of the phenotypic variation) located in the interval of *Xbarc1118-Xbarc105* on chromosome 4D was detected in seven environments. The high frequency of the QTL in this region suggested that this chromosome interval was important for TGW QTLs for GNS which were detected on 12 chromosomes, such as 1A, 1D, 2B, 2D, 4A, 4B, 5A, 5B, 5D, 6B, 7A, and 7D, previously (Hai et al. 2008; Marza et al. 2006; Cuthbert et al. 2008; Wang et al. 2009; McIntyre et al. 2010). In this study, two QTLs (*QGns-2B1* and *QGns-2B2*, explained 4.56–6.91 and 5.29–5.44 % of the phenotypic variation) were mapped on chromosome 2B in four environments. Hai et al. (2008) also reported two QTLs (*QGne.nfcri-2B.1* and *QGne.nfcri-2B.2*) for GNS on the same chromosome. We also found that *QGns-4B*, explained 6.33–14.25 % of the phenotypic variation, linked with *Xbarc20* on chromosome 4B was consistent with QTL mapping results of Marza et al. (2006) and Wang et al. (2011). FNS shows positive correlation with GNS, suggesting that FNS is important for yield. Wang et al. (2011) detected a stable QTL for FNS on chromosome 4A in an $F_{2:3}$ population. In this study, we identified a QTL near the gene-specific marker, *ANT*, across seven environments, which may coincide with previous reports by Wang et al. (2011). Therefore, we postulated that *TaANT* gene could be a candidate gene for QTL controlling FNS. These QTLs that could be detected both in our and other studies may exist truly, and they could be used in MAS directly.

On the other hand, most of the QTLs contributed by Zang 1817 were novel QTLs that have not been reported by other studies. It was probably because that few previous studies were focused on QTL mapping using Tibetan semi-wild wheat as one of the parents, and Tibetan semi-wild wheat may have some specific alleles in these loci. And

these novel QTLs from Zang 1817 that could be detected in more than three environments, such as *QSl-7A1*, *QEp-4B2*, *QGws-4D* and *QTgw-4D*, may be used in improvement of relevant traits utilizing Zang 1817 as a superior gene resource in future wheat molecular breeding.

QTL-rich regions and pleiotropic effects

The existence of QTL-rich regions in wheat genome has been reported in previous studies (Quarrie et al. 2005; Marza et al. 2006; Huang et al. 2006; Kumar et al. 2007), whereas few were focused on yield-related traits. In this study, we found that QTLs controlling yield-related traits were also not randomly distributed on chromosome, and some QTLs were identified and concentrated in certain regions on chromosomes 4A, 4B and 4D (Fig. 1, Supplemental Table 5). For example, stable QTLs controlling five yield-related traits, such as SL, SSN, GWE, FNS and GNS, were detected in the interval of *Xwmc491-Xwmc96* on chromosome 4A. In particular, the positive alleles for the QTLs underling both FNS and GNS in this region were contributed by the female parent ND3331. Moreover, these two traits showed significant positive correlation, the co-localization of the QTLs controlling these traits may suggest that they could be controlled by the same genes. We also found that QTLs controlling all of the nine traits analyzed could be detected in the interval of *Xbarc20-Xbarc1174b* on chromosome 4B. It is interesting that all the positive alleles of QTLs for FSN, FNS and GNS in this region were contributed by ND3331, suggesting that there may be the same QTL (s)/gene (s) responsible for all the three traits or FSN and FNS only and ultimately these two could lead to increased GNS. There is also a QTL cluster for PH, SL, GNS, SSN, GWS, and FNS located between *Xbarc340* and *Xksm154* which was mapped on chromosome 4B. Another QTL-rich region detected on 4B is adjacent to the marker Xcau603, in which stable QTLs for the three related traits TGW, GNS and GWS were detected. All the positive alleles for these QTLs were controlled by ND3331 in these two regions mentioned above. It seems that QTLs for correlated traits tend to cluster together on chromosome. Another stable QTL cluster was detected for TGW and GWS, which is between *Xbarc105* and *Xbarc217* on 4D, and the positive alleles were from Zang 1817, the existence of QTL-rich region for yield-related traits in the homoeologous group 4 suggested that these chromosomes may have experienced artificial selection during the past breeding practices.

Functional marker and marker-assisted selection

QTL mapping would play a vital role in molecular marker-assisted breeding. The using of gene-specific markers or functional markers is proven to be more efficient. The co-linearity of genomic sequence and the conservation of homologue genes in different cereal crops, such as rice, maize, wheat, sorghum and *Brachypodium*, could facilitate the cloning and functional characterization of important genes of wheat (Peng et al. 1999), and can be used to develop paralogous gene-specific marker in wheat. In this study, the strategy was used to develop *TaANT* gene-specific marker and *TaANT* was mapped on chromosome 4A where the QTLs controlling FNS, SL, SSN, GWP and GNS have been identified.

ANT gene is a member of *AP2* gene family, and involved in the formation of flower. Mutation of *ANT* gene in *Arabidopsis* leads to male sterility, while overexpression enlarges the reproductive organs of *Arabidopsis*, including flower, legume and seed (Krizek 1999; Mizukami and Fischer 2000). *TaANT* gene has also been reported to take part in the development of floral organ, and may play a decisive role in grain number per spike of wheat (Mizumoto et al. 2009). In this study, *TaANT* was mapped in the interval of *Xksm71-Xcfd6* on chromosome 4A, and the genetic distance between *TaANT* and the two makers was 0.1 and 0.7 cM, respectively. Furthermore, QTLs controlling FNS, FSN, GNS and GWS were also identified in the same region.

Acknowledgments This work was financially supported by the Major Program of the National Natural Science Foundation of China (31290210) and 863 Project of China (2012AA10A309).

Authors' contributions Gang Liu performed the whole experiment and drafted the manuscript, Lijia Jia and Lahu Lu performed the phenotypic analysis of the RILs population, Dandan Qin performed the mapping of the TaANT gene, Jinping Zhang and Panfeng Guan performed the genotyping of the RILs population, Zhongfu Ni and Yingyin Yao analyzed the data, Qixin Sun and Huiru Peng designed the experiment and revised the manuscript. All authors have read and approved the final manuscript.

Conflict of interest We declare that we have no financial and personal relationships with other people or organizations that can inappropriately influence our work, and all of the authors declare that they have no conflict of interests.

Ethical standards All of the authors have read and have abided by the statement of ethical standards for manuscripts submitted to Theoretical and Applied Genetics.

References

Bernacchi D, Beck-Bunn T, Eshed Y, Lopez J, Petiard V, Uhlig J, Zamir D, Tanksley S (1998) Advanced backcross QTL analysis in tomato. I. Identification of QTLs for traits of agronomic importance from *Lycopersicon hirsutum*. Theor Appl Genet 97:381–397

Brown LR (1994) State of the World. Norton, New York

Carter AH, Garland-Campbell K, Kidwell KK (2011) Genetic mapping of quantitative trait loci associated with important

agronomic traits in the spring wheat (*Triticum aestivum* L.) cross 'Louise' × 'Penawawa'. Crop Sci 51:84–95

Cui F, Ding AM, Li J, Zhao CH, Wang L, Wang XQ, Qi XL, Li XF, Li GY, Gao JR, Wang HG (2012) QTL detection of seven spike-related traits and their genetic correlations in wheat using two related RIL populations. Euphytica 186:177–192

Cui F, Zhao CH, Li J, Ding AM, Li XF, Bao YG, Li JM, Ji J, Wang HG (2013) Kernel weight per spike: what contributes to it at the individual QTL level? Mol Breed 31:265–278

Cui F, Zhao CH, Ding AM, Li J, Wang L, Li XF, Bao YG, Li JM, Wang HG (2014) Construction of an integrative linkage map and QTL mapping of grain yield-related traits using three related wheat RIL populations. Theor Appl Genet 127:659–675

Cuthbert JL, Somers DJ, Brûlé-Babel AL, Brown PD, Crow GH (2008) Molecular mapping of quantitative trait loci for yield and yield components in spring wheat (*Triticum aestivum* L.). Theor Appl Genet 117:595–608

Deng SM, Wu XR, Wu YY, Zhou RH, Wang HG, Jia JZ, Liu SB (2011) Characterization and precise mapping of a QTL increasing spike number with pleiotropic effects in wheat. Theor Appl Genet 122:281–289

Eujayl I, Sorrells M, Baum M, Wolters P, Powell W (2001) Assessment of genotypic variation among cultivated durum wheat based on EST-SSRs and genomic SSRs. Euphytica 119:39–43

Gaynor RC (2010) Quantitative Trait Loci Mapping of Yield, its Related Traits, and Spike Morphology Factors in Winter Wheat (*Triticum aestivum* L.). Gaynor RC for the degree of Master of Science in Crop Science presented on May 27, 2010

Hai L, Guo HJ, Wagner C, Xiao SH, Friedt W (2008) Genomic regions for yield and yield parameters in Chinese winter wheat (*Triticum aestivum* L.) genotypes tested under varying environments correspond to QTL in widely different wheat material. Plant Sci 175:226–232

Hayes PM, Liu BH, Knapp SJ, Chen F, Jones B, Blake T, Franckowiak J, Rasmusson D, Sorrells M, Ullrich SE, Wesenberg D, Kleinhofs A (1993) Quantitative trait locus effects and environmental interaction in a sample of North American barley germplasm. Theor Appl Genet 87:392–401

Heidari B, Sayed-Tabatabaei BE, Saeidi G, Kearsey M, Suenaga K (2011) Mapping QTL for grain yield, yield components, and spike features in a doubled haploid population of bread wheat. Genome 54(6):517–527

Huang XQ, Cloutier S, Lycar L, Radovanovic N, Humphreys DG, Noll JS, Somers DJ, Brown PD (2006) Molecular detection of QTLs for agronomic and quality traits in a doubled haploid population derived from two Canadian wheats (*Triticum aestivum* L.). Theor Appl Genet 113:753–766

Krizek BA (1999) Ectopic expression of AINTEGUMENTA in *Arabidopsis* plants results in increased growth of floral organs. Dev Genet 25:224–236

Kumar N, Kulwal PL, Balyan HS, Gypta PK (2007) QTL mapping for yield and yield contributing traits in two mapping populations of bread wheat. Mol Breed 19:163–177

Ladizinsky G (1985) Founder effect in crop-plant evolution. Econ Bot 39:191–199

Li SS, Jia JZ, Wei XY, Zhang XC, Li LZ, Chen HM, Fan YD, Sun HY, Zhao XH, Lei TD, Xu YF, Jiang FS, Wang HG, Li LH (2007) An intervarietal genetic map and QTL analysis for yield traits in wheat. Mol Breed 20:167–178

Liao XZ, Wang J, Zhong RH, Ren ZL, Jia JZ (2008) Mining favorable alleles of QTLs conferring 1,000 grain weight from synthetic wheat. Acta Agron Sin 34:1877–1884 (in Chinese with English abstract)

Lincoln S, Daly M, Lander E (1992) Mapping genes controlling quantitative traits with MAPMAKER/QTL, Version 1.1 In: a tutorial and reference manual, 2nd edn. Whitehead Institute Technical Report 46, Cambridge

Marza F, Bai GH, Carver BF, Zhou WC (2006) Quantitative trait loci for yield and related traits in the wheat population Ning7840 × Clark. Theor Appl Genet 112:688–698

McIntyre CL, Mathews KL, Rattey A, Chapman SC, Drenth J, Ghaderi M, Reynolds M, Shorter R (2010) Molecular detection of genomic regions associated with grain yield and yield-related components in an elite bread wheat cross evaluated under irrigated and rainfed conditions. Theor Appl Genet 120:527–541

Mir RR, Kumar N, Jaiswal V, Girdharwal N, Prasad M, Balyan HS, Gupta PK (2012) Genetic dissection of grain weight in bread wheat through quantitative trait locus interval and association mapping. Mol Breed 29:963–972

Mizukami Y, Fischer RL (2000) Plant organ size control: AINTEGUMENTA regulates growth and cell numbers during organogenesis. Pro Natl Acad Sci 97:942–947

Mizumoto K, Hatano H, Hirabayashi C, Murai K, Takumi S (2009) Altered expression of wheat AINTEGUMENTA homolog, WANT-1, in pistil and pistil-like transformed stamen of an alloplasmic line with *Aegilops crassa* cytoplasm. Dev Genes Evol 219(4):175–187

Moncada P, Martinez CP, Borrero J, Châtel M, Gauch H Jr, Guimaraes E, Tohmé J, McCouch SR (2001) Quantitative trait loci for yield and yield components in an Oryza sativa × Oryza rufipogon BC_2F_2 population evaluated in an upland environment. Theor Appl Genet 102:41–52

Peng JH, Fahima T, Röder MS, Li YC, Dahan A, Grama A, Ronin YI, Korol AB, Nevo E (1999) Microsatellite tagging of the striperust resistance gene YrH52 derived from wild emmer wheat, *Triticum dicoccoides*, and suggestive negative crossover interference on chromosome 1B. Theor Appl Genet 98:862–872

Peng JH, Ronin Y, Fahima T, Röder MS, Li YC, Nevo E, Korol A (2003) Domestication quantitative trait loci in *Triticum dicoccoides*, the progenitor of wheat. Proc Natl Acad Sci 100:2489–2494

Pestsova E, Ganal MW, Röder MS (2000) Isolation and mapping of microsatellite markers specific for the D genome of bread wheat. Genome 43:689–697

Quarrie SA, Steed A, Calestani C, Semikhodskii A, Lebreton C, Chinoy C, Steele N, Pljevljakusić D, Waterman E, Weyen J, Schondelmaier J, Habash DZ, Farmer P, Saker L, Clarkson DT, Abugalieva A, Yessimbekova M, Turuspekov Y, Abugalieva S, Tuberosa R, Sanguineti MC, Hollington PA, Aragués R, Royo A, Dodig D (2005) A high-density genetic map of hexaploid wheat (*Triticum aestivum* L.) from the cross Chinese Spring × SQ1 and its use to compare QTLs for grain yield across a range of environments. Theor Appl Genet 110:865–880

Quarrie SA, Quarrie SP, Radosevic R, Rancic D, Kaminska A, Barnes JD, Leverington M, Ceoloni C, Dodig D (2006) Dissecting a wheat QTL for yield present in a range of environments: from the QTL to candidate genes. J Exp Bot 57(11):2627–2637

Ramya P, Chaubal A, Kulkarni K, Gupta L, Kadoo N, Dhaliwal HS, Chhuneja P, Lagu M, Gupta V (2010) QTL mapping of 1,000-kernel weight, kernel length, and kernel width in bread wheat (*Triticum aestivum* L.). J Appl Genet 51:421–429

Röder MS, Korzun V, Wendehake K, Plaschke J, Tixier MH, Leroy P, Ganal MW (1998) A microsatellite map of wheat. Genetics 149:2007–2023

Sheng H, See DR, Murray TD (2012) Mapping QTL for resistance to eyespot of wheat in *Aegilops longissima*. Theor Appl Genet 125:355–366

Somers DJ, Isaac P, Edwards K (2004) A high-density microsatellite consensus map for bread wheat (*Triticum aestivum* L.). Theor Appl Genet 109:1105–1114

Sun QX, Ni ZF, Liu ZY, Gao JW, Huang TC (1998) Genetic relationships and diversity among Tibetan wheat, common wheat and European spelt wheat revealed by RAPD markers. Euphytica 99:205–211

Sun XC, Marza F, Ma HX, Carver BF, Bai GH (2010) Mapping quantitative trait loci for quality factors in an inter-class cross of US and Chinese wheat. Theor Appl Genet 120:1041–1051

Tanksley SD, McCouch SR (1997) Seed banks and molecular maps: unlocking genetic potential from the wild. Science 277:1063–1066

Tanksley SD, Grandillo S, Fulton TM, Zamir D, Eshed T, Petiard V, Lopez J, Beck-Bunn T (1996) Advanced backcross QTL analysis in a cross between an elite processing line of tomato and its wild relative *L. pimpinellifolium*. Theor Appl Genet 92:213–224

Wang XN (2010) Genetic analysis of quantitative traits in RIL population derived from common wheat and semi-wild Tibetan wheat. Wang XN for the degree of master of crop science presented on June, 2010

Wang GL, Mackill DJ, Bonman JM, McCouch SR, Champoux MC, Nelson RJ (1994) RFLP mapping of genes conferring complete and partial resistance to blast in a durably resistant rice cultivar. Genetics 136:1421–1434

Wang RX, Hai L, Zhang XY, You GX, Yan CS, Xiao SH (2009) QTL mapping for grain filling rate and yield related traits in RILs of the Chinese winter wheat population Heshangmai × Yu8679. Theor Appl Genet 118:313–325

Wang JS, Liu WH, Wang H, Li LH, Wu J, Yang XM, Li XQ, Gao AN (2011) QTL mapping of yield-related traits in the wheat germplasm 3228. Euphytica 177:277–292

Xie W, Ben-David R, Zeng B, Distelfeld A, Röder MS, Dinoor A, Fahima T (2012) Identification and characterization of a novel powdery mildew resistance gene PmG3M derived from wild emmer wheat, *Triticum dicoccoides*. Theor Appl Genet 124:911–922

Yang Y, Zhao XL, Xia LQ, Chen XM, Xia XC, Yu Z, He ZH (2007) Development and validation of a Viviparous-1 STS marker for pre-harvest sprouting resistance in Chinese wheats. Theor Appl Genet 115:971–980

Zeng ZB (1993) Theoretical basis for separation of multiple linked gene effects in mapping quantitative trait loci. Pro Natl Acad Sci 90:10972–10976

Zeng ZB (1994) Precision mapping of quantitative trait loci. Genetics 136(4):1457–1468

Zhang DL, Hao CY, Wang LF, Zhang XY (2012) Identifying loci influencing grain number by microsatellite screening in bread wheat (*Triticum aestivum* L.). Planta 236:1507–1517